RAPID COMMUNICATIONS

PHYSICAL REVIEW B VOLUME 44, NUMBER 15 15 OCTOBER 1991-I

Sensitivity of conductance fluctuations to the addition of single elastic scatterers in mesoscopic GaAs/$Al_xGa_{1-x}As$ heterostructures

S. J. Klepper,* O. Millo, M. W. Keller, and D. E. Prober*
Department of Applied Physics, Yale University, New Haven, Connecticut 06520

R. N. Sacks
United Technologies Research Center, East Hartford, Connecticut 06108
(Received 19 March 1991; revised manuscript received 7 June 1991)

We have studied magnetoconductance fluctuations in mesoscopic wires fabricated from GaAs/$Al_xGa_{1-x}As$ heterostructures. By photoionizing *DX* centers in the $Al_xGa_{1-x}As$, we controllably alter the elastic-scattering configuration of our devices. A technique of conductance-fluctuation difference traces allows us to quantitatively study changes to the characteristic device fluctuations. The amplitude and temperature dependence of these conductance changes agree well with theory. We can also resolve switching events in device conductance due to the effect of adding a single scatterer.

A number of electron-transport effects involving quantum phase coherence have come to light in recent years. The phenomenon of "universal" conductance fluctuations (UCF) in diffusive mesoscopic systems, in particular, has led to many additional insights.[1] (Diffusive electron motion occurs when the elastic-scattering length l is much smaller than the sample dimensions.) An intriguing prediction of the theory is that the conductance of a phase-coherent system will be significantly changed by the movement of even a *single* impurity.[2,3] Movement of a single elastic scatterer alters the quantum interference of all Feynman paths that visit the scattering site. This sensitivity to the position of a single impurity might open the way to utilizing conductance fluctuations as a microscopic probe of the defect dynamics of individual impurity atoms.

Evidence for the sensitivity of conductance to the motion of single scatterers is found in observations of two- and multilevel fluctuators in a variety of systems. Spontaneous switching events have been seen in the conductance of Si metal-oxide-semiconductor field-effect transistor devices,[4] in very thin films of Bi (Ref. 5) and other disordered metals, in GaAs devices,[6] and in extremely narrow (and hence nondiffusive) normal-metal constrictions.[7] Other work in GaAs shows the production of a large number of distinct switchers in a heterojunction after the application of a voltage pulse.[8] Noise studies done on thin films of Bi demonstrate the effect of superposition of many switchers.[9] Much of this work can be understood in terms of conductance-fluctuation theory. Unfortunately, experimental control over, and detailed knowledge of, the impurity dynamics in those devices was generally lacking.

What we have accomplished is to *controllably* alter the elastic-scattering configuration in a diffusive mesoscopic device, and to test the single-scatterer predictions[2,3] in a more quantitative and rigorous manner. The alteration of the scattering configuration is made possible by the existence of deep donor levels in $Al_xGa_{1-x}As$, known as *DX* centers.[10-13] These are in the Si-doped layer adjacent to the two-dimensional electron gas (2DEG) in our GaAs/$Al_xGa_{1-x}As$ heterostructures. A *DX* center in the ground state can be photoionized using sub-band-gap infrared (IR) light;[11] this has the effect of adding an elastic scatterer to a heterojunction device. As discussed later, this is equivalent to *moving* an elastic scatterer or impurity, the situation treated by the theory.[2,3] Once added, this extra scatterer remains fixed until the device is annealed to temperatures above 100 K.[11] Thus there are no intrinsic impurity dynamics at low temperatures, so these devices are model systems in which to study single-scatterer effects.

We have carried out two kinds of experiments. In the first, we study the change in magnetoconductance after illumination with a fixed IR dose which adds N scatterers. From this change we may determine both the amplitude and the temperature dependence of the rms conductance change δG_1, due to adding a *single* elastic scatterer. The second type of experiment involves the search for discrete conductance shifts due to individual ionization events, *while* the device is illuminated.

The rms amplitude for the conductance change δG_1 due to the movement of a single impurity atom by a distance δr is predicted to be,[3] at $T=0$,

$$(\delta G_1)^2 \approx \left(\frac{e^2}{h}\right)^2 \left(\frac{\Omega}{N_i l^2}\right) \alpha(k_F \delta r) .$$

N_i is the number of scatterers present in the sample, Ω is the area equal to $L \times W$, and l is the elastic mean free path. α measures the change of electron phase due to the motion of a scatterer, and saturates at unity for $\delta r > k_F^{-1}$. Our calculations indicate that $\alpha = 1$ for our experiment, as discussed below. All of the ionized donors adjacent to the conducting layer contribute their electrons to the 2DEG; these ions are the dominant elastic scatterers,[12] so $(N_i/\Omega) = n$; n is the 2D electron density. The finite temperature result for the relative conductance shift $(\delta G_1/G)^2$ in a 2DEG device is

$$\left(\frac{\delta G_1}{G}\right)^2 = 2\pi C^2 \left(\frac{e^2}{h}\right)^2 R_\square^2 \left(\frac{1}{nl^2}\right) \left(\frac{L_\phi^2}{LW}\right)^2 \left(\frac{L_T}{L_\phi}\right)^2 .$$

L_ϕ is the phase-coherence length and $L_T \equiv (\hbar D/k_B T)^{1/2}$ is the thermal length. This equation includes the effects of thermal averaging and of classically adding conductance fluctuations from phase-coherent regions of the wire with $L, W > L_\phi$. Finally, using $k_F = \sqrt{2\pi n}$ we obtain

$$\frac{\delta G_1}{G} = 2\pi C \left(\frac{e^2}{h}\right) R_\square \left(\frac{1}{k_F l}\right) \left(\frac{L_\phi L_T}{LW}\right). \quad (1)$$

The constant C is of order unity[1] and is determined from our UCF magnetoconductance data to be $C \approx 0.97$. The corresponding UCF amplitude is[1]

$$\frac{\delta G_{\rm UCF}}{G} = \sqrt{2\pi} C \left(\frac{e^2}{h}\right) R_\square \left(\frac{L_T}{\sqrt{LW}}\right). \quad (2)$$

Devices were fabricated by chemically etching a GaAs/$Al_{0.3}Ga_{0.7}As$ heterojunction grown by molecular-beam epitaxy without an undoped $Al_xGa_{1-x}As$ spacer layer. The ~400-Å-thick $Al_xGa_{1-x}As$ layer was uniformly doped with Si at a concentration of 1×10^{18} cm^{-3}; a 215-Å GaAs cap layer protects the structure. The elimination of the undoped spacer layer ensures that the devices have low mobility (~25000 cm^2/Vs) and small elastic-scattering length $l \approx 0.4$ μm, so that they are in the regime of diffusive electron transport. A typical wire is 22 μm in total length between outer voltage probes and is 3 μm wide. Only the mesoscopic region is illuminated, since the leads are covered with a grounded metal IR shield. Electron concentration for devices cooled in the dark is $n \approx 9\times10^{11}$ cm^{-2}, with sheet resistance $R_\square \approx 300$ Ω. Shubnikov-de Haas data indicate that only the first subband of the 2DEG is occupied. The thermal length $L_T \approx 0.8$ μm ($T^{-1/2}$), with T in K. Low-field magnetoresistance data analyzed[14] using weak-localization theory yields values for $L_\phi \approx 2.6$ μm ($T^{-1/2}$) and for the spin-orbit scattering length $L_{\rm SO} \approx 1.7$ μm. The $T^{-1/2}$ temperature dependence of L_ϕ and its magnitude indicate that quasielastic electron-electron scattering[15] is the predominant phase breaking mechanism in the temperature range 1.2–8 K studied. Data are presented below for two samples, A and B, which were fabricated from different wafers.

Calibrations for the rate of DX center photoionization were made on large, unshielded Hall bar devices. Our infrared light-emitting diode (LED) had peak emission at 930 nm at 300 K. Measurement of the rate of change of the Hall voltage V_H at a fixed magnetic field for a given LED current yielded a value for the rate of change of the electron concentration n given by

$$(dn/dt) = -(n/V_H)(dV_H/dt)$$
$$\approx (1.0\pm0.2)\times10^{-4}\mu{\rm m}^{-2}{\rm s}^{-1}\mu{\rm A}^{-1}.$$

Recall that $n \approx 9\times10^3$ μm^{-2}. Through IR illumination of our samples, we can randomly alter the microscopic scattering configuration at a controlled average rate.

Figure 1 shows magnetoconductance traces at $T = 3$ K for sample A, (a) before and (b) after IR illumination which added $N \approx 25000$ scatterers to the device. The rms deviation of each trace from its average is just $(\delta G_{\rm UCF}/G)$. The magnetoconductance measurement after

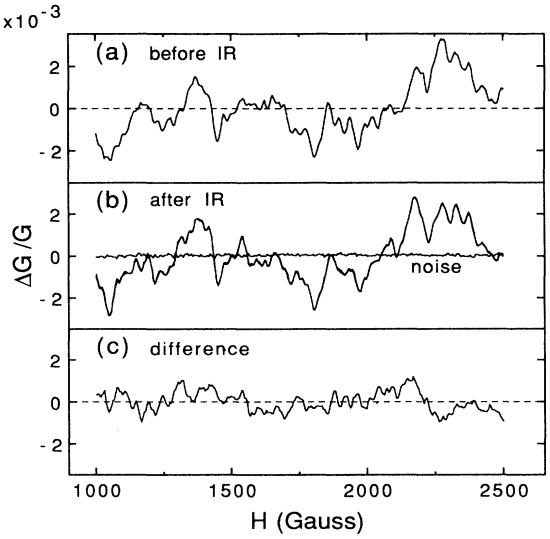

FIG. 1. Magnetoconductance traces for sample A at 3 K; $\Delta G \equiv G(T) - G_{\rm av}$. (a) Curve taken before IR illumination. (b) Overlapping traces labeled "after IR" were both taken after a period of illumination which added $N \approx 25000$ scatterers; their difference, labeled "noise," is comparable to the directly measured system noise. (c) The difference between the magnetoconductance traces obtained before and after illumination.

illumination was repeated. Figure 1(b) displays the two "after IR" traces and their difference, labeled noise, which shows the total noise of the sample and the measuring system. The stability of this noise trace demonstrates that the scattering configuration of our device indeed remains fixed after IR exposure. We subtract the traces of Figs. 1(a) and 1(b) to obtain a "difference trace," Fig. 1(c). By the ergodic hypothesis,[1] the rms deviation of this difference trace from its average, taken over a magnetic-field range large compared to the correlation field[1] H_C, is δG_N. In practice we use $N \gg 1$ to obtain readily measurable changes and to reduce the fractional statistical uncertainty in N, of $N^{-1/2}$. We choose N small enough, however, that $\delta G_N < \delta G_{\rm UCF}$. δG_1 is then given by

$$\delta G_1 = \delta G_N/\sqrt{N}, \quad (3)$$

which holds for the addition of N random changes.

Figure 2 shows the temperature dependences of δG_1 and of $\delta G_{\rm UCF}$ for sample B and the predictions of Eqs. (1) and (2). To obtain $\delta G_{\rm UCF}$, the magnetoconductance was measured at several temperatures. The device was then exposed to IR illumination in which $N \approx 2000$ elastic scatterers were added, and the UCF traces were remeasured. The difference traces were computed to obtain δG_N. The predicted temperature dependences of δG_1 and $\delta G_{\rm UCF}$ are determined by L_T and L_ϕ; each length is $\propto T^{-1/2}$. From the *difference-trace* amplitude we find, for all of our measurements, that $(\delta G_1/G) \propto T^{(-1.0\pm0.2)}$; this agrees with the dependence in Eq. (1) of $(\delta G_1/G) \propto L_\phi L_T \propto T^{-1}$. The experimental UCF amplitude is $(\delta G_{\rm UCF}/G) \propto T^{(-0.5\pm0.1)}$; this agrees with the $T^{-1/2}$ dependence in Eq. (2).

To examine the dependence of δG_N on the number of

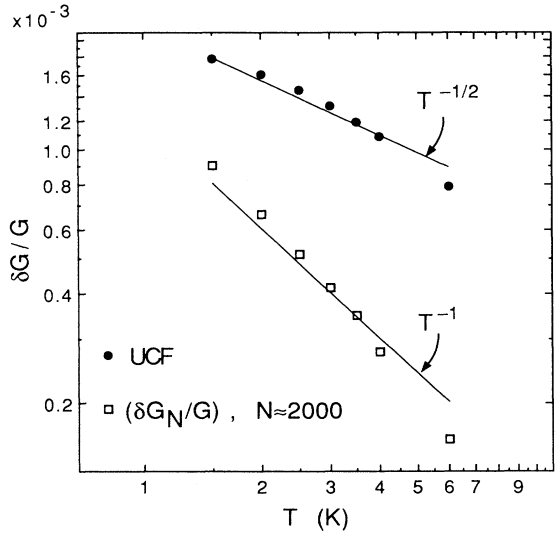

FIG. 2. Temperature dependence of the rms amplitudes of the UCF and of the difference traces corresponding to $N \approx 2000$ added scatterers for sample B. Note the T^{-1} behavior of the difference traces, and the $T^{-1/2}$ behavior of the full fluctuations, as indicated by the solid lines.

added scatterers N and to establish its magnitude accurately, we illuminated a device a number of times with a fixed dose of IR radiation and computed difference traces between all combinations of magnetoconductance curves. In Fig. 3, the square amplitude of the difference traces, $(\delta G_N/G)^2$, is plotted as a function of N for sample B at 2.5 K. Equation (3) gives $(\delta G_N/G)^2 = N(\delta G_1/G)^2$. Our data in Fig. 3 confirm this linear dependence; we find that

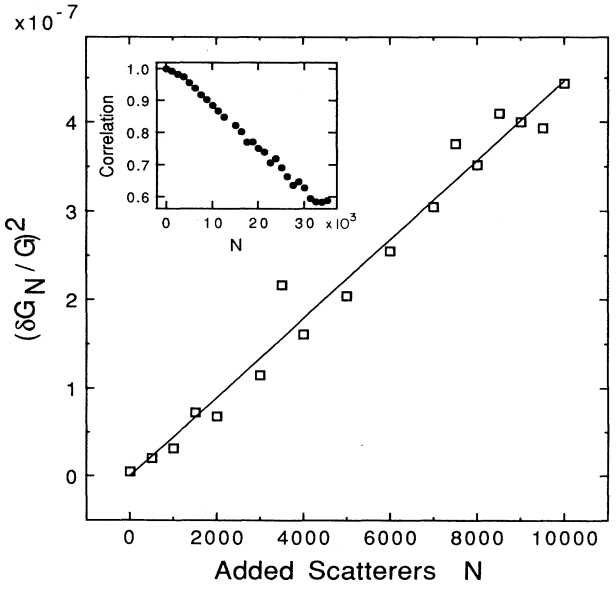

FIG. 3. Dependence of the square amplitude of the difference traces on the number of added scatterers, for sample B. From the slope of the best-fit (solid) line, we infer $(\delta G_1/G)$. Inset: Correlation between fluctuation traces decreases with the addition of scatterers. For both plots, $T = 2.5$ K.

$(\delta G_N/G)^2 \propto N^{(1.0 \pm 0.1)}$. From the best linear fit in Fig. 3, we find $(\delta G_1/G)$ (experiment) $= 6.7 \times 10^{-6}$, compared to a calculated value of $(\delta G_1/G)$ (theory) $= 7.9 \times 10^{-6}$. In general we find agreement with theory to within 25% for the values of $(\delta G_1/G)$ determined in this way. The same data are displayed in a different manner in the inset of Fig. 3, which shows decreasing correlation[1] between UCF traces as scatterers are added.

Decorrelation of the conductance-fluctuation traces (to a correlation coefficient of 0.5), and approach of δG_N to the value $\delta G_{\rm UCF}$, can be achieved through the addition of a sufficiently large number of scatterers, N_C:

$$N_C \approx (\delta G_{\rm UCF}/\delta G_1)^2 = N_i(l^2/L_\phi^2) .$$

For sample B this gives $N_C \approx 30000$ at $T = 2.5$ K, out of a background number of scatterers $N_i \approx 600000$. N_C is larger in device A. For $N \approx N_C$, we do find both the expected decorrelation and the expected value of δG_N.

It is possible to look directly at conductance changes *during* IR illumination, as individual DX centers are ionized. An example of such data for sample B is presented in the upper trace in Fig. 4, between the dashed lines; outside the dashed lines, there is no illumination. Several points are noteworthy. Theory predicts the rms value $\delta G_1/G$; what is seen in our measurement is the distribution of conductance changes which results in this rms value. The vertical bar in Fig. 4 is the size of $\delta G_1/G$ calculated from Eq. (1). Since this value is only a factor of 3 above the peak-to-peak noise, we expect a significant fraction of the smaller changes to be obscured by noise. The switching events evident in Fig. 4 are comparable in size to $\delta G_1/G$. On average, ten such events should occur in the time indicated by the horizontal bar labeled "10 τ" in Fig. 4. About one-third this many events can be resolved. We attribute this discrepancy to the large number of switching events which are concealed in the noise. The lower trace in Fig. 4 shows the conductance of the unilluminated device; it is stable, but shows some system noise.

A critical tenet of our analysis is that ionizing a DX

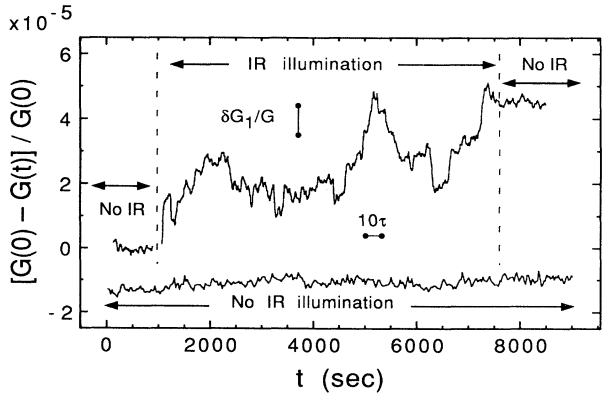

FIG. 4. Conductance for sample B under weak IR illumination (between the dashed lines in the upper trace) and unilluminated (outside the dashed lines and lower trace). Switching events compare in amplitude to the rms value from theory, $\delta G_1/G$. We expect to observe ten events in the time marked "10τ." The lower curve is offset for clarity.

center is equivalent to moving an impurity. There are two issues. First, does the added positive charge of an ionized *DX* center affect conductance fluctuations as would an impurity which changed position? Second, what effect does the electron added to the 2DEG by photoionization have on the quantum conductance? We begin with the first question. Ionized *DX* centers are the background elastic scatterers present in our heterojunctions.[12] Photoionizing a *DX* center is equivalent to *adding* an elastic scatterer. The random potential which the conduction electrons see is modified; due to screening, this change of potential occurs over a relatively short distance, ≈ 10 nm. Our semiclassical calculations show that electron phases along paths near the added scatterer are increased by $> 2\pi$ because of the locally changed potential. In addition, the electron phases change due to the changed impurity configuration. In terms of the effect on electron phase, adding a scatterer to a device is therefore equivalent to moving an impurity by a distance $\delta r > k_F^{-1}$. This is equivalent to the impurity motion treated by theory with $\alpha = 1$. A small decrease to the Drude conductivity does result from each added scatterer. This Drude term, however, is subtracted out in our difference-trace analysis. It does bias our data under IR illumination in the direction of decreased conductance, but is smaller than δG_1.

The second issue, the effect of the added electron, is more subtle. Each ionized *DX* center adds an electron to the 2DEG. The added electron increases the carrier density locally around the ionized donor. We conducted experiments to determine whether the conductance-fluctuation effects we observe could be due to the increase of the *average* electron density, rather than the *localized* potential changes discussed above. We studied a device, sample *C*, in which an electrical gate extends over the sample region. A gate voltage V_g was applied to uniformly change the electron density n; the change is $\Delta n \propto V_g$. We find that the rms conductance change is $(\delta G)^2 \propto V_g^2 \propto (\Delta n)^2$. This is consistent with predictions for the dependence on k_F of the quantum conductance.[1] In the photoionization experiments, the increase in average electron density is given by $\Delta n \approx N/LW$, with N the number of photoionized *DX* centers. For photoionization in samples *A* and *B*, we find, as expected,[3] that $(\delta G)^2 \propto \Delta n$ (see Fig. 3). This different dependence on Δn proves that the conductance-fluctuation effects we observe for photoionization are due predominantly to the induced changes in the random elastic-scattering potential, and not to a change in k_F. Thus photoionizing a *DX* center is fully equivalent to the movement of an impurity.

To summarize, we are able to alter the elastic-scattering configuration in a mesoscopic wire in a controlled manner. We have studied in detail the evolution of the characteristic magnetoconductance fluctuations brought about by the addition of scatterers, using a difference-trace technique. The value we obtain for the average conductance shift δG_1 that results from adding a single scatterer to a device agrees well with theory both in its amplitude and in its temperature dependence. We are also able to resolve changes in the sample conductance due to the addition of a single scatterer.

The authors acknowledge the advice and assistance of P. D. Dresselhaus and R. G. Wheeler, as well as useful discussions with A. D. Stone, B. L. Al'tshuler, Y. Imry, and S. Feng. Facilities of the Yale Center for Microelectronics Materials and Structures were used. Funding for this work was provided by NSF Grant No. DMR-8505539 and by Yale University; O.M. was supported by the Weizmann Foundation.

*Also at Department of Physics.

[1] P. A. Lee, A. D. Stone, and H. Fukuyama, Phys. Rev. B **35**, 1039 (1987), and references therein.

[2] B. L. Al'tshuler and B. Z. Spivak, Pis'ma Zh. Eksp. Teor. Fiz. **42**, 363 (1985) [JETP Lett. **42**, 447 (1985)].

[3] S. Feng, P. A. Lee, and A. D. Stone, Phys. Rev. Lett. **56**, 1960, 2772(E) (1986).

[4] K. S. Ralls, W. J. Skocpol, L. D. Jackel, R. E. Howard, L. A. Fetter, R. W. Epworth, and D. M. Tennant, Phys. Rev. Lett. **52**, 228 (1984); W. J. Skocpol, P. M. Mankiewich, R. E. Howard, L. D. Jackel, D. M. Tennant, and A. D. Stone, *ibid.* **56**, 2865 (1986).

[5] D. E. Beutler, T. L. Meisenheimer, and N. Giordano, Phys. Rev. Lett. **58**, 1240, 2608(E) (1987).

[6] G. M. Gusev, Z. D. Kvon, E. B. Olshanetsky, V. Sh. Aliev, V. M. Kudriashov, and S. V. Palessky, J. Phys. Condens. Matter **1**, 6507 (1989).

[7] K. S. Ralls and R. A. Buhrman, Phys. Rev. Lett. **60**, 2434 (1988).

[8] D. Mailly, M. Sanquer, J.-L. Pichard, and P. Pari, Europhys. Lett. **8**, 471 (1989).

[9] N. O. Birge, B. Golding, and W. H. Haemmerle, Phys. Rev. Lett. **62**, 195 (1989).

[10] D. V. Lang and R. A. Logan, Phys. Rev. Lett. **39**, 635 (1977).

[11] T. N. Theis and S. L. Wright, Appl. Phys. Lett. **48**, 1374 (1986).

[12] E. Calleja, P. M. Mooney, S. L. Wright, and M. Heiblum, Appl. Phys. Lett. **49**, 657 (1986).

[13] A. Kastalsky and J. C. M. Hwang, Solid State Commun. **51**, 317 (1984).

[14] O. Millo, S.J. Klepper, M. W. Keller, D. E. Prober, S. Xiong, A. D. Stone, and R. N. Sacks, Phys. Rev. Lett. **65**, 1494 (1990).

[15] B. L. Al'tshuler, A. G. Aronov, and D. E. Khmel'nitskii, J. Phys. C **15**, 7367 (1982).